Biophysical Journal Volume 68 February 1995 483–490

The Conductance of the Muscle Nicotinic Receptor Channel Changes Rapidly upon Gating

David J. Maconochie, George H. Fletcher, and Joseph H. Steinbach
Department of Anesthesiology, Washington University School of Medicine, St. Louis, Missouri 63110 USA

ABSTRACT We have recorded single-channel currents through fetal-type muscle nicotinic receptor channels at recording bandwidths of approximately 50 and 75 kHz. The time course of the rising phase of aligned and averaged openings can be entirely accounted for if it is assumed that the conductance of the single channel changes instantaneously, and that alignment and averaging introduce a dispersion of 2–3 μs. We conclude that we find no evidence for a gradual change in conductance as a channel opens or closes. The shapes of averaged power spectra are consistent with this conclusion, insofar as they exclude an exponential relaxation in the transition with a time constant of 10 μs or more.

INTRODUCTION

In most analyses of channel gating, activation is modeled as a process involving discrete kinetic states (cf. Hodgkin and Huxley, 1952; Stevens, 1972), and it is assumed that the transition between two states is instantaneous. If, as Eyring (1936) suggests, transitions between two states proceed by way of an unstable intermediate, reaction rates reflect the probability of there being sufficient energy to reach the intermediate, whereas the lifetime of the intermediate is short and the time spent in transit brief. When the transition involves a structural change such as the opening of an ion channel, it is less clear that the time spent in transit can be considered brief, or that the change in conductance is instantaneous.

Previous studies of the initiation and cessation of current flow through individual nicotinic receptor channels have indicated that the *measured* rate of change in current flow is restricted by the frequency response of the measuring apparatus (Hamill et al., 1981; Sigworth, 1986). However, these analyses were performed using data filtered at 10 kHz or less. From a comparison of the time course of the current to the system step response, Hamill et al. (1981) concluded that their data were incompatible with the idea that "the open-close transitions were spread out in time over 10 μs or more." Other authors have reported a more complicated time course for the opening and closing of channels (Auerbach and Sachs, 1984; Ferguson et al., 1993). They find that channels pass through states of differing conductance so that the time course of the averaged transition is prolonged. Ferguson et al. (1993) found that large conductance Ca^{2+}-activated K^+ channels often do not open directly to the full single-channel conductance. The initial opening in a burst is often to a brief duration "subconductance" state. A brief duration subconductance state has also been reported to occur on the initial opening of some bursts of muscle nicotinic receptors (Auerbach and Sachs, 1984), although this observation has not been made in other studies (Auerbach and Sachs, 1983, 1984; Sigworth, 1986).

Because the state of a channel protein is normally inferred from the current flowing through the channel, a relatively slow conductance change would limit our ability to estimate kinetic parameters for channel gating. Some recent estimates of the apparent rate for channel opening (that is, the rate for going from a closed to an open state) for the nicotinic receptor channel approach the limit set by Hamill et al. (1981): 30,000 s^{-1} (frog muscle at 11°C; Colquhoun and Sakmann, 1985), 45,000 s^{-1} (*Torpedo* receptors expressed in fibroblasts, 22°C; Sine et al., 1990), and 60,000 s^{-1} (mouse muscle receptors expressed in fibroblasts, 22°C; Maconochie and Steinbach, 1992).

We have reexamined the time course of the change in current flow through single muscle nicotinic receptors at improved temporal resolution, to revise the limit on the time taken for this channel to switch between being fully closed and fully open.

MATERIALS AND METHODS

Recordings

Single-channel currents were recorded from cell-attached patches (Hamill et al., 1981) on cultured fibroblasts that express the fetal form of the mouse muscle nicotinic receptor (Kopta and Steinbach, 1994). Cells were depolarized to near zero transmembrane potential with a high K^+ bath saline (140 mM KCl, 1.0 mM $MgCl_2$, 2.0 mM EGTA, 20 mM HEPES, pH 7.3). The pipette solution contained 140 mM KCl, 5 mM glucose, 20 mM HEPES (pH 7.3), and either 200 or 400 nM ACh. Data were obtained at room temperature (22–24°C), using pipettes pulled from borosilicate glass (KG-33) and coated with Sylgard (Dow-Corning, Midland, MI). Pipette resistances were 3–5 MΩ.

All data were obtained using a List EPC-7 patch clamp, with no internal filters set. Data were obtained using either the 0.5 GΩ feedback resistor (greater bandwidth), or the 50 GΩ feedback resistor (better signal-to-noise ratio). 1 s segments of data were acquired at 1 MHz (DAS50; Keithley-Metrabyte, Taunton MA) and transferred to disk. Usually 10 segments of data were sampled, with single-channel openings occurring at a rate of 10 to 50 s^{-1}. All analyses were performed on a 80486-based personal computer,

---

Received for publication 1 June 1994 and in final form 10 August 1994.

Address reprint requests to J. H. Steinbach, Department of Anesthesiology, Washington University School of Medicine, 660 S. Euclid, St. Louis, MO 63110. Tel.: 314-362-8564; Fax: 314-362-8571; E-mail: jhs@morpheus.wustl.edu.

0006-3495/95/02/483/08 $2.00

using VIEWMENU (available from the U.S. military software database SIMTEL, as DELPX03).

System impulse response

The electrical characteristics of the recording system are often obtained by applying a test signal to a wire placed close to, but separated from the headstage input by an air gap (Hamill et al., 1981). The signal is differentiated by the "air gap" capacitor so that a triangular test waveform results in a current step into the headstage input, whereas a step will result in a current impulse. We adopted a similar approach to measure the system impulse response while recording in the cell-attached configuration: we applied a voltage step between the bath and signal ground. In the cell-attached configuration, the resistance between the recording pipette and the bath is tens of GΩ, whereas the capacitance between pipette and bath is a few pF. A voltage step imposed between the bath and signal ground, therefore, results in a brief pulse of current being applied to the interior of the pipette through the pipette-to-bath capacitance in combination with the cell membrane and patch capacitances, with a negligible contribution passing through the seal resistance (see Fig. 2, *A* and *D*). We chose to measure the system impulse response in the cell-attached recording configuration, because it can be expected that the interposition of a pipette between a signal (such as that coming from a membrane patch) and the headstage input might modify the overall transfer function.

Estimates of the recording bandwidth using the 50 GΩ resistor are around 50 kHz (−3 dB; see Results). We also estimated the bandwidth by the more conventional method in which a step is applied to an air-gap capacitor between a wire and the silver wire electrode in the pipette holder, and found the recording bandwidth to be slightly wider (around 60 kHz; data not shown). With the 0.5 GΩ resistor the bandwidth recording cell-attached is around 75 kHz (see Results), whereas using the air-gap capacitor the bandwidth is about 100 kHz.

Data selection, alignment, and averaging

Averages were made from unfiltered records. Sections of data containing suitable channel transitions were extracted from the record if the opening lasted at least 1 ms with no closings visible in the filtered record, and was preceded (for openings) or followed (for closings) by a closed period lasting at least 1 ms with no openings visible (Fig. 1). Hence, openings that lasted less than 1 ms (i.e., "brief openings"; cf. Lingle et al., 1992) were not analyzed. Similarly, brief closings were not analyzed.

Transitions were aligned using digitally filtered data and a 50% threshold crossing method. The threshold was calculated from the means of 100–500 μs segments before and after a provisional estimate for the midpoint of the transition. The alignment point was determined by the first point in the filtered record to cross a threshold set halfway between the two mean values. Filtered records were used for alignment, to ensure that threshold crossings due to noise did not lead to a spurious setting of the alignment point. However, the averages were made from unfiltered data.

Digital filtering for alignment

Time series data were filtered by convolution with an appropriate filter (the time series representation of the filter transfer function). We employed a modified version of "optimal" or Wiener filtering (Press et al., 1992). Wiener filtering produces the closest approximation in a *least-squares sense* to a given signal waveform for a known noise spectral density. The description of the filter in the frequency domain is

$$T = \{|SR|^2\}/\{|SR|^2 + |NR|^2\},$$

where S is the the frequency domain representation of the signal of interest, N is the expected noise, and R is the transfer function of the apparatus. The modified noise power spectrum $|NR|^2$ was estimated by averaging power spectra of sections of data that did not appear to have any single-channel events. The averaged power spectrum was further smoothed by representation as an arbitrary polynomial. The modified signal power spectrum $|SR|^2$ was calculated as follows. We assumed the signal to be a step function of the appropriate size (the single-channel current amplitude) and calculated its power spectrum S. To calculate SR we multiplied S by an approximation to R, a function that was constant to the headstage bandwidth, and then rolled off rapidly (i.e., faster than the measured R). The advantage of this approximation is that it avoids significant contributions to T at high frequencies (above the roll-off of the amplifier) at which N is essentially unknown. The time domain filter coefficients were obtained by reverse Fourier transformation of T, and the coefficients truncated above insignificant terms (10^4 times smaller than the largest term) by a raised cosine window.

Estimating the dispersion in alignment

Some error in the estimation of the alignment point is unavoidable, and will result in some dispersion of the time course of the averaged record. It is also possible to increase the rate of rise of the averaged record above the true rate if high frequency noise components are artificially synchronized by the alignment procedure.

To investigate these effects, we synthesized some data using defined signals with noise added as follows. We estimated the background power spectrum from sections of real data that included no single-channel openings visible by eye in the filtered record. This average of 50 power spectra was converted into background noise by taking the square root of the amplitude and randomizing the phase of each frequency component. The result was then inverse-transformed to obtain the time series background noise record. To this was added a 12 point ramp, a step or an integrated system impulse response of the same size as the single-channel current (the integrated impulse response is the step response). By repeating the randomization of the phase of each frequency component, 100 unique synthetic records of each of the three signal types plus noise were generated.

We analyzed the synthetic data in the identical fashion to real data. We used a filtered record to establish a point for alignment, and then averaged the 100 unfiltered records. By repeating the process of alignment and averaging with a range of different filters, we were able to come to two empirical conclusions. First, the filter type that leads to the least dispersion of the data, either step or ramp, is a Wiener filter. Second, to avoid a spurious alignment of high frequency noise components (visible as a distortion of the ramp), it is necessary to filter records sufficiently that the time derivative does not change sign during the rising phase of the current. (With some data, it was necessary to reduce the expected amplitude of the single-channel step to a fraction in the range of 0.5–0.7 of the actual value to achieve this.)

In making these tests, we also obtained an idea of the dispersion introduced by the alignment procedure. We know beforehand that the true alignment point is identical for every synthesized data record. Therefore, the SD of the *calculated* alignment point gives us the dispersion introduced by our analysis. The dispersion estimated this way is 2–3 μs for each of the synthesized signals.

Modeling the time course of averaged single-channel transitions

If we hypothesize that the single-channel opening event is a step, then our data record should consist of a step convolved with the system impulse response. However, we have noted above that we cannot align data perfectly, and the least dispersion due to misalignment that we might expect is of the order of 2–3 μs. Hence, we tested the hypothesis that our data record is the average of many steps, each modified by the system impulse response and imperfectly aligned. We assumed that the misalignment can be represented by a Gaussian distribution, and used a Levenberg-Marquardt routine to find the SD of the misalignment. In practice we obtained a test signal from a convolution of an integrated Gaussian with the measured system impulse response, and minimized the sum of the squared differences between the test signal and our data record. Four parameters were adjusted: the Gaussian mean value (mean alignment point) and SD (σ, the error in alignment), and two scaling parameters (the amplitude of the integrated Gaussian and a constant current offset). The parameter of interest is $\underline{\sigma}$, the best-fitting estimate of the SD.

To generate the test signal, the integrated Gaussian was calculated at one-third μs intervals, and numerically convolved with the system impulse response. The impulse response and the averaged data record were linearly interpolated at one-third μs intervals. We found that the fitting procedure failed to converge when σ became less than 0.7 μs because of the discrete nature of the signals involved, so in these cases that value is reported (see Table 1).

It is important to place some limits on the estimate for $\underline{\sigma}$. Changes in σ result in changes to the residual that are roughly symmetrical about the middle of the rising phase of the averaged current, and of opposite sign (see Fig. 3). To estimate the range of values for σ that could describe a given averaged opening, the best-fitting integrated Gaussian was determined as described above. The value for σ was then systematically stepped while the other parameters were held constant. The record was divided into segments before and after the middle of the transition, and the residuals in the two segments compared by way of their means and SDs. The null hypothesis is that an adequate value for σ would produce mean residuals in the previous and subsequent segments that did not differ significantly from each other, as evaluated from a Student's *t*-test. The value for σ was considered inappropriate for describing the averaged transition if the two mean residuals were sufficiently different ($p < 0.05$ that they were drawn from the same population). In some cases a lower limit for σ could not be obtained with this approach, as the value for p remained above 0.05 at the smallest value of σ tested (0.24 μs).

We tested this procedure by synthesizing 100 records consisting of the integrated system impulse response plus noise, as described above and shown in Fig. 3 *B*.

Power spectra

Power spectra were calculated using fast Fourier transforms of time series data. The system transfer function was obtained as the Fourier transform of the impulse response, calculated for a square-windowed segment starting at the foot of the impulse response. We show in Fig. 4 the averages of many power spectra of the impulse responses, which are estimates of the modulus squared of the system transfer function ($|T_S|^2$). The background spectra for subtraction were taken from periods when no channel openings were discernible by eye in the Wiener-filtered record.

Records containing transitions were selected for spectral analysis as described earlier (see Data selection and alignment). As described above, channel opening and closing transitions are hypothesized to resemble a step. For comparison to the power spectra of the system impulse response, data were first digitally differentiated by replacing the current at sample point n $\{I(n)\}$ with the difference $\{I(n+1) - I(n-1)\}$. Signal power spectra, the spectra of differentiated segments containing a single opening or closing transition, were calculated with equal numbers of points either side of the alignment point, to include equal closed and open channel periods. Similarly, background noise spectra were obtained from equal numbers of differentiated data segments when a channel was open and when a channel was closed. The segments were Hann-windowed. Difference spectra were obtained by subtraction of background noise spectra from signal spectra.

If the signal consists not of a step but a relaxation (modified by the system transfer function), then this might be apparent in the difference power spectrum. We calculated power spectra predicted for exponential relaxations with time constants of 1, 3, and 10 μs, by multiplying the amplitudes of the predicted Lorentzian and the smoothed spectra of the system impulse responses. The test functions were scaled to match the data between 2 and 6 kHz, and we then performed a signs test on data in the range 6–23 kHz (at the upper limit, the signal-to-noise ratio in the spectra was sufficiently reduced that half of the spectra analyzed included negative values of the difference power). The test determined whether the distribution of data points around the test function differed significantly from the predictions of a binomial distribution with an equal probability that the points lay above or below. The criterion for adequate fit was that the number of points above the predicted curve should lie within the 0.95 confidence interval predicted from the null hypothesis.

RESULTS

Aligned and averaged channel openings and closings

We recorded data with no internal filter set in the patch clamp amplifier, at a 1 μs sampling interval. A section of data with three channel openings (*upwards deflections*) is shown in Fig. 1 *A*, recorded with the 0.5 GΩ feedback resistor, at a holding potential of −100 mV. Superimposed on the data is a filtered representation, in which the openings are more

TABLE 1 Results of fitting the time course of averaged openings and closings

			Openings				Closings			
Record	V (mV)	R (GOhm)	N	$\underline{\sigma}$ (μs)	σ_l (μs)	σ_u (μs)	N	$\underline{\sigma}$ (μs)	σ_l (μs)	σ_u (μs)
13–1.1	−50	50	270	2.2		4.9	303	2.4	1.2	3.5
13–1.2	−100	50	210	2.3	1.9	2.8	255	2.5	1.4	3.5
13–1.3	−100	0.5	181	0.7*		2.3	171	4.0	1.9	5.9
13–1.4	−150	0.5	163	2.3		3.7	178	2.3		4.5
12–1.1	−100	50	86	1.3		1.9	110	1.6		2.3
12–1.2	−100	0.5	91	0.7*		2.3	56	0.7*		4.5
12–1.3	−150	50	58	2.7	1.9	4.0	92	1.8	0.7	2.8
12–4.1	−100	50	162	0.7*		1.9	99	2.0		3.0
12–4.2	−100	0.5	115	2.4		2.1	109	0.7*		3.0
12–4.3	−150	50	69	0.7*		2.1	55	1.9		2.1
12–21.1	−100	50	60	1.8	1.2	2.8	65	3.0	2.6	3.5
Mean				1.6		2.8		2.1		3.5
SD				0.8		1.0		1.0		1.1

We give values for the patch membrane potential (V), the feedback resistor value (R), and the number of transitions averaged (N). The parameters given are the SD of the least-squares best fitting integrated Gaussian ($\underline{\sigma}$), and the estimated lower (σ_l) and upper (σ_u) limits (see Materials and Methods). In some cases as $\underline{\sigma}$ tended toward 0 the fitting procedure became unstable, so a value of 0.7 μs (denoted by an asterisk) was assigned to allow convergence. Arithmetic mean values and SDs were computed including values of 0.7 μs. The value for σ_l was undefined if the p value had not decreased to 0.05 at $\sigma = 0.24$ μs (denoted by a dash).

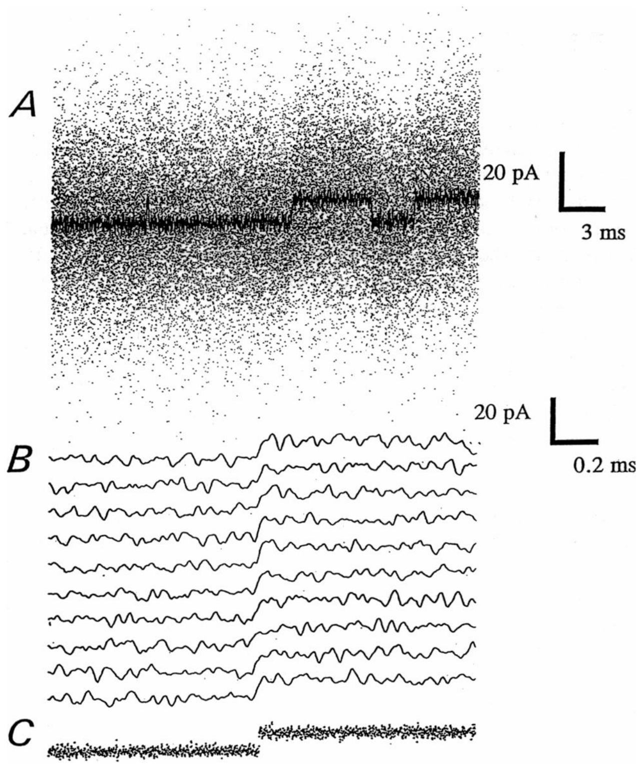

FIGURE 1 Alignment and averaging of single-channel currents. (*A*) A short section of raw data recorded from a cell-attached patch on a Q-F18 cell, in which three channel openings can be seen (*upwards deflections*). The data are shown as recorded, with no filtering, and overlaid with the results of digitally filtering with a Wiener filter (see Materials and Methods). (*B*) 10 selected data segments from this record, in which the opening of a channel was preceded by a period of at least 1 ms with no openings and the channel remained open for at least 1 ms. These data have been filtered and aligned on the midpoint of the transition in the filtered record. (*C*) Average of 181 aligned opening events from this patch, made from unfiltered data. Data were collected with the 0.5 GΩ feedback resistor, digitized at 1 MHz, pipette potential +100 mV, 400 nM ACh in the pipette. Filtering performed with assumed step size 70% of the measured single-channel amplitude. (Record 13-1.3).

apparent. Ten opening transitions filtered with a modified Wiener filter and aligned on the midpoint of the transition (see Materials and Methods) are shown in Fig. 1 *B*, at an expanded time scale. The data were selected on the basis that there are no openings visible during the closed period before the transition, and no closings visible during the open period after the transition. The result of averaging many unfiltered records is shown in Fig. 1 *C*. Each trace was aligned using a filtered record (as shown in Fig. 1 *B*), but the average was constructed from unfiltered data. As can be seen, the averaged opening appears nearly instantaneous on this time scale.

We examined the averaged opening and closing transitions more closely, as indicated in Fig. 2. We do not have in mind any particular function to describe the time course of a transition. We therefore tested the hypothesis that the averaged time course arises from many instantaneous steps, each modified by the system transfer function and imperfectly aligned. Panels *A* and *D* of Fig. 2 show the system impulse response (the response to a pulse of current applied to the pipette as described in Materials and Methods) for the two headstage resistors, on the same time scale. We assumed that the error in alignment follows a Gaussian distribution, and fit to the averaged data record a signal consisting of an integrated Gaussian convolved with the measured impulse response (see Materials and Methods). The parameter of interest is the SD ($\underline{\sigma}$) of the Gaussian distribution that produced the best-fitting test signal, which we use to define the dispersion in alignment of the steps. The smooth traces superimposed on the averaged transitions in Fig. 2, *B*, *C*, *E*, and *F* are the best-fitting test signals. The estimates for $\underline{\sigma}$ are summarized in Table 1: for openings the mean dispersion is 1.6 ± 0.8 μs (mean ± SD, 11 data sets from 4 patches), whereas for closings it is 2.1 ± 1.0 μs. The difference between estimates for openings and closings is not significant ($p > 0.2$ from a two-tailed *t*-test). There do not appear to be any systematic variations with the size of the feedback resistor or the membrane potential, and the value for $\underline{\sigma}$ is comparable with our estimate of the dispersion introduced in our alignment procedure (see Materials and Methods).

We also examined the effect of various values of σ on the ability of the test signal to describe the data (see Materials and Methods). Fig. 3 *A* shows an averaged opening transition (*thick line*) with a superimposed best-fitting test signal (*thin solid line*; $\underline{\sigma}$ of 2.7 μs). The difference between the averaged opening and the best fit is plotted below, so that the residuals can be compared in the segments before and after the midpoint of the opening. The residuals in these two segments did not differ from each other, as assessed from Student's *t*-test ($p = 0.5$; see Materials and Methods). To set limits on the estimate of $\underline{\sigma}$, we systematically varied the value of σ and compared the residuals in the segments before and after the midpoint. The two dashed lines represent the signals predicted with σ of 1.9 or 4.0 μs, for which the probabilities that the differences in the residuals arose by chance were 0.03 and 0.01, respectively. The lower limit for $\underline{\sigma}$, therefore, is 1.9 μs, and the upper limit is 4.0 μs. Values for other data sets are given in Table 1. Also shown in Fig. 3 *A* is the signal predicted with σ set to 10 μs (*dotted line*), which is clearly inconsistent with our data.

Fig. 3 *B* shows the results of an identical analysis on synthesized data. Using the procedure described in Materials and Methods (estimating the dispersion in alignment), we constructed 100 records with the identical noise spectral density as the data in Fig. 3 *A*. The underlying signal was a system step response of the same amplitude as the single-channel currents of Fig. 3 *A* and was obtained by integrating the system impulse response recorded from the same cell attached patch as the data in Fig. 3 *A*. We have the advantage, with synthesized data, of knowing in advance the real location of the simulated transition. Thus, we also know the dispersion introduced by the alignment procedure. For this data set, it was 2.3 μs. The value of $\underline{\sigma}$ obtained from the best-fitting test signal was 3.0 μs, with lower and upper limits of 1.9 μs ($p = 0.03$) and 3.8 μs ($p = 0.03$). These estimates of the dispersion are internally consistent, suggesting both

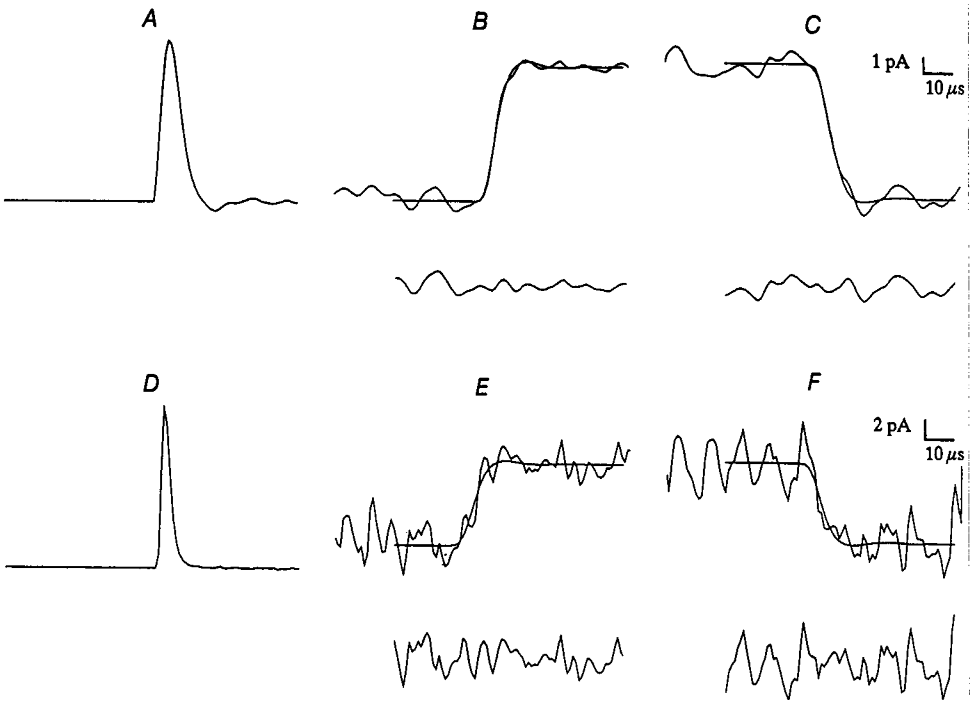

FIGURE 2 The time course of averaged single-channel opening and closing events. Traces *A–C* were recorded with the 50 GΩ feedback resistor in the patch clamp amplifier, whereas traces *D–F* were recorded with the 0.5 GΩ feedback resistor. Traces *A* and *D* show the system impulse response (see Materials and Methods). Parts *B*, *C*, *E*, and *F* show averages of selected, aligned single-channel opening or closing transitions; an upwards deflection indicates an opening event. Averages were made from unfiltered data, after alignment (see Materials and Methods and Fig. 1). Each trace is overlaid with a fitted function. The function is obtained from the measured impulse response of the system and a theoretical curve representing an average of square opening events dispersed with a Gaussian distribution that has SD σ (see Materials and Methods). In practice an integrated Gaussian was convolved with the system impulse response and parameters adjusted to minimize the sum of squared deviations from the data. The smoother curves shown in parts *B*, *C*, *D*, and *F* show the best-fitting curves, with the residuals plotted underneath the data at the same scale. The fits shown in parts *C* and *E* had values for $\underline{\sigma}$ of 2.0 and 2.4 μs, respectively. For the data shown in parts *B* and *F*, the fitting procedure became unstable as the value of σ became very small (see Materials and Methods), so σ was set to a value of 0.7 μs to obtain the fit shown. Data were recorded at a transmembrane potential of −100 mV, parts *A–C* with the 50 GΩ feedback resistor and parts *D–F* with the 0.5 GΩ resistor. The number of individual responses averaged was: A, 11; B, 111; C, 111; D, 11; E, 115; F, 109. (Records 12-4.1 and 12-4.2.).

that the approach we have taken for estimating $\underline{\sigma}$ works and that the shape of the averaged data record can be accounted for by the modification of a step in current by the electronic characteristics of the recording system and the imperfect alignment of many individual data records.

Spectra of segments containing an opening or closing transition

A second approach, which does not rely on the data being precisely aligned, is to examine power spectra of data sections containing a channel opening or closing transition and compare them with the frequency response of the recording system. To improve the signal-to-noise ratio, we averaged together spectra obtained from both openings and closings. We begin with the hypothesis that a data segment in which there is a transition contains a signal in the form of a step plus noise, modified by the properties of the recording system. The data were differentiated so that the postulated step becomes an impulse, and the power spectrum of the differentiated data should consist of the spectrum of the system impulse response plus the background noise spectrum. The background noise spectrum was obtained from differentiated data segments that did not contain a transition, and subtracted from the spectra of segments containing transitions. To balance the contribution of fluctuations in closed- and open-channel periods, the spectra of records with transitions were computed with the transition centered in the window, and background spectra were computed from equal numbers of segments with no channels open and one channel open (see Materials and Methods).

The results of applying this approach are shown in Fig. 4. Fig. 4, *Ai* and *Bi* show the averaged power spectra of differentiated records, and Fig. 4, *Aii* and *Bii* show the difference spectra. The spectra of the matching impulse responses are shown in Fig. 4, *Aiii* and *Biii*. The hypothesis, as described in the frequency domain, is that the spectra of the differentiated single-channel transition, after background noise has been subtracted (Fig. 4, *Aii* and *Bii*), should be identical to the spectra of the impulse responses (Fig. 4, *Aiii* and *Biii*). The spectra are similar in that the power is constant with frequency to a frequency of about 30 kHz. Above 30 kHz there is so much scatter that it is difficult to draw a conclusion.

We examined the difference spectra further to see to what extent they supported the hypothesis of the single-channel

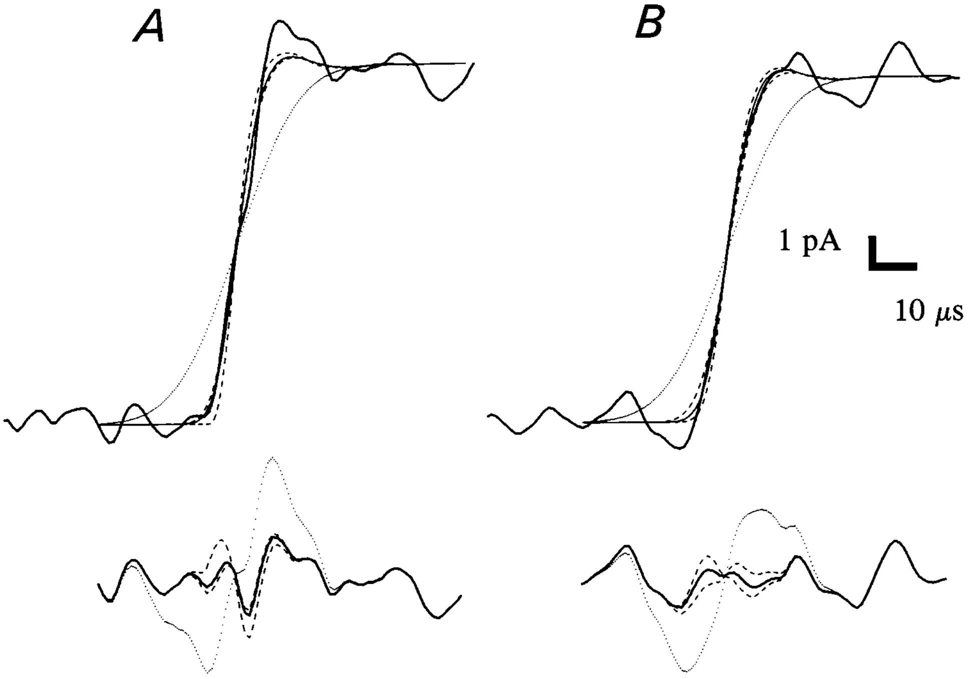

FIGURE 3 Putting limits on the fitted value of the dispersion. An average of 58 unfiltered single-channel openings is shown in part *A thick solid line*). It is overlaid with the best-fitting predicted curve (*thin solid line*), for which $\underline{\sigma} = 2.6$ μs. The residuals are plotted below at the same scale. To put limits on this value, different values of σ were tried, keeping the other parameters constant. The residuals to either side of the midpoint were compared, and an estimate made of the probability, p, that the residuals arose from the same population (see Materials and Methods). The dashes indicate curves for which $\sigma = 1.9$ μs ($p = 0.03$) or $\sigma = 4.0$ μs ($p = 0.02$). The dots follow a curve for which $\sigma = 10$ μs ($p < 10^{-6}$). Data recorded at −150 mV, 50 GΩ feedback resistor, average of 58 openings. (Record 12-1.3.). In part *B*, the same process has been repeated for synthesized data with the identical noise spectral density, and with a signal consisting of the system step response scaled to the single-channel amplitude. The thick line shows the average of 100 unique synthesized records. In performing the alignment, the SD between the calculated alignment point and the known midpoint of the original signal is 2.3 μs. The average was made from unfiltered synthesized records, which had been aligned exactly as actual data were. The value of $\underline{\sigma}$ is 3.0 μs, and the dashed lines indicate curves for which $\sigma = 1.9$ μs ($p = 0.03$) and $\sigma = 3.8$ μs ($p = 0.03$).

transition being a step. If there were an exponential relaxation present, the spectral density of the transition should take on a characteristic shape of a Lorentzian multiplied by the squared modulus of the the system transfer function ($|T_S|^2$). Overlaid in Fig. 4, *Aii* and *Bii* are the curves predicted for exponential relaxation time constants of 1, 3, and 10 μs. Inspection of the figure suggests immediately that a curve predicted by a time constant of 10 μs does not agree with the data. The same is true for 10 out of 11 of our data sets. We used a signs test to see if the observed scatter of data points around the predicted curves could have arisen by chance (see Materials and Methods). In summary, six out of seven data sets recorded with the 50 GΩ feedback resistor and two of four data sets recorded with the 0.5 GΩ feedback resistor failed the signs test for the 10 μs relaxation: more data points lay above the curve than are predicted to have arisen by chance. On the other hand, only one of the data sets obtained with the 50 GΩ resistor and none of the data sets obtained with the 0.5 GΩ resistor showed any significant deviation from 1 or 3 μs predicted curves. These observations indicate that single-channel transitions are unlikely to follow an exponential time course with a time constant as long as 10 μs. The poor signal-to-noise ratio above 30 kHz prevents us from drawing the same conclusion for relaxation time constants of 1 and 3 μs.

DISCUSSION

Our observations indicate that the conductance of channels of muscle nicotinic receptor changes very rapidly when the channel opens. Hamill et al. (1981) presented the results of an analysis of the average of six openings recorded at a bandwidth of 10 kHz and reached the same conclusions. We have extended these results with a more extensive data set obtained at wider bandwidth.

We find that to account for the time course of averaged transitions, we need to assume that there is some dispersion of the single-channel transition, of the order of 2–3 μs. This degree of dispersion is identical to the variation in the alignment point predicted from synthesized data of the identical single-channel amplitude and noise spectral density. We conclude, therefore, that there is no need to hypothesize any other mechanism to account for the observed dispersion (σ) of the averaged single-channel transition and that the change in conductance takes place in less than 3 μs.

To avoid the question of dispersion due to alignment, we also examined the spectral density of the opening and closing transitions. We came to much the same conclusion, that if the transitions followed an exponential time course, then the time constant certainly has to be less than 10 μs and probably is not much more than 3 μs.

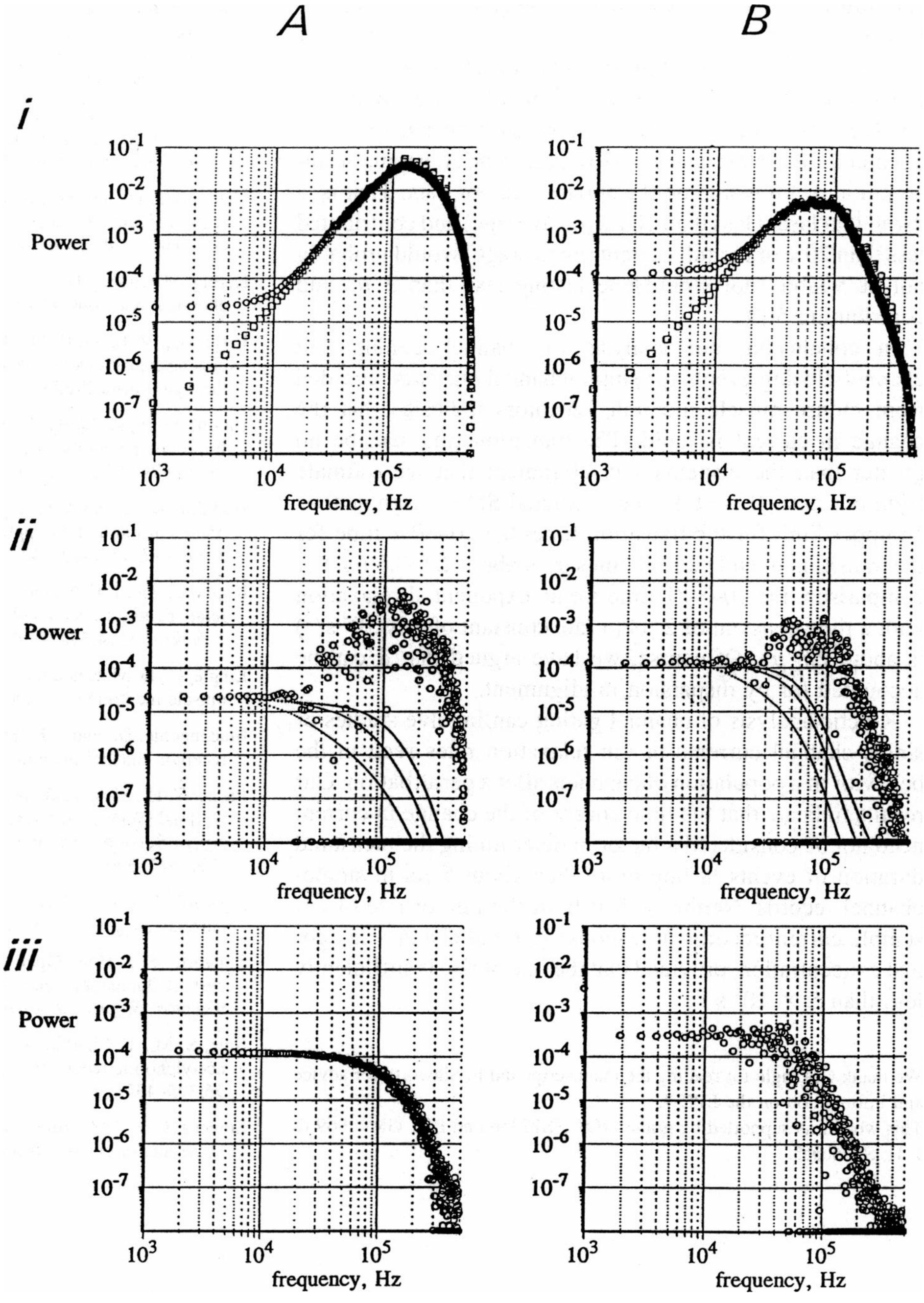

FIGURE 4 An alignment-independent analysis of single-channel opening and closing transitions. Power spectra are shown for data obtained with the 0.5 GΩ resistor (column *A*) and the 50 GΩ resistor (column *B*). Power (in arbitrary units) is plotted against frequency. Averaged spectra are shown in row (*i*), computed from differentiated data records that contained a transition (○) and that did not (□). The difference spectra are shown in row (*ii*) (○). Frequencies at which the difference in power spectra was negative are shown by points plotted on the abscissa. Overlaid in row (*ii*) are spectra predicted from exponential functions with time constants of 10, 3, and 1 μs, modified by the appropriate system transfer function, T_S (*thin lines*). The spectra of the system impulse responses, which are estimates of $|T_S|^2$, are shown in row (*iii*). The predicted curves shown in row (*ii*) were compared with the spectra using a signs test (see Materials and Methods). For data obtained with the 0.5 GΩ feedback resistor (column *A*), 17 of 18 points lay above the curve predicted by the 10 μs time constant, and 11 points above the 3 μs and 1 μs curves. With the 0.5 GΩ resistor (column *B*), 16 of 18 points lay above the curve predicted by the 10 μs curve, 12 points for the 3 μs curve and 11 points for the 1 μs curve. The 0.95 confidence limits for the binomial equation are 4 points to 14 points. The spectra shown in *Ai* are the averages of spectra from 341 differentiated records containing transitions and 682 background records recorded at −150 mV (record 13-1.4). The spectra shown in *Bi* are the averages from 91 differentiated records containing transitions and 182 background records recorded at −150 mV (record 12-1.3). The spectrum in *Aiii* is the average of 21 spectra of system impulse responses, with the average of 84 background noise spectra subtracted. The spectrum in *Biii* is the average of 11, with the average of 44 background noise spectra subtracted.

Other authors have also examined averaged opening and closing transitions of nicotinic receptor channels, although at lower bandwidth. In three studies, the goal was to determine whether in opening or closing, channels often passed through states with a conductance different from the full open state. Auerbach and Sachs (1983, 1984) analyzed data from chick primary myotubes in culture, with conflicting results. In one patch (Fig. 10 of Auerbach and Sachs, 1984), essentially every burst began and ended with a subconductance dwell, although analysis of other data sets showed no indication that subconductance states occurred frequently at the beginning or end of a burst (Auerbach and Sachs, 1983, 1984). However, Sigworth (1986) examined averaged opening and closing transitions in data obtained using cultured rat myotubes and found that the time courses followed the system step response (data filtered at 2 or 4 kHz). He was particularly interested in determining whether there was evidence for the occurrence of a subconductance that is relatively close to the main conductance level, based on his analysis of the excess noise present during current flow through nicotinic receptor channels opened by low concentrations of ACh (Sigworth, 1985). He found that the noise could be described by a model in which the channel conductance fluctuated by about 3%, with a relaxation time constant of about 1 ms at 10°C. The averaged openings and closings, however, showed no sign that channels either opened into or closed from a particular conductance level. The variability of these observations on the occurrence of subconductance states indicates that some care must be taken in extrapolating results from one preparation to another.

Our data obtained with mouse fetal receptors expressed in fibroblasts also do not show any signs of a dwell in a subconductance state during the transition between the fully open and fully closed states. However, a brief, small, or uncommon dwell would not be apparent in our data. That is, a dwell that lasted less than 10 μs (on average) and contributed less than 20% of the full current (on average) would probably not be visible, nor would one lasting less than 3 μs and contributing 50%.

In conclusion, our analysis of channel-opening and channel-closing events for single-channel currents recorded from mouse muscle nicotinic receptors indicates that the change in current is rapid. The transition time can be no greater than the dispersion in alignment that we estimate from our data. If we take the estimated SD of alignment as an upper limit for the transition time, the 20–80% time for the transition would be 1.68 times $\underline{\sigma}$, or about 2.5–3.5 μs. For comparison, the 20–80% time for an exponential relaxation with a time constant of 2 μs (a rate constant of 5×10^5 s^{-1}) is about 2.8 μs. Of course, we have argued that $\underline{\sigma}$ can be accounted for by dispersion in alignment.

Kinetic analysis of channel gating can involve studies of single-channel currents or the relaxation rates seen in the behavior of a population of channels after a perturbation. Our results indicate that the time course of the change in current need not be considered a factor in determining the measured duration of events lasting more than about 5 μs in single-channel records. Neither will it limit the rate of rise of ensemble current records in response to rapid changes in agonist concentration, provided that the rate of rise is sufficiently less than 5×10^5 s^{-1}.

We thank C. Lingle for reading the manuscript and F. Sigworth for advice and information on the EPC-7.

This work was supported by grants RO1 NS22356 and PO1 GM47969 to J. H. Steinbach.

REFERENCES

Auerbach, A., and F. Sachs. 1983. Flickering of a nicotinic ion channel to a subconductance state. *Biophys. J.* 42:1–10.

Auerbach, A., and F. Sachs. 1984. Single channel currents from acetylcholine receptors in embryonic chick muscle: kinetic and conductance properties of gaps within bursts. *Biophys. J.* 45:187–198.

Colquhoun, D., and B. Sakmann. 1985. Fast events in single-channel currents activated by acetylcholine and its analogues at the frog muscle end-plate. *J. Physiol.* 369:501–557.

Eyring, H. 1936. The activated complex and the absolute rate theory of chemical reactions. *Chem. Rev.* 17:65–77.

Ferguson, W. B., O. B. McManus, and K. L. Magleby. 1993. Opening and closing transitions for BK channels often occur in two steps via sojourns through a brief lifetime subconductance state. *Biophys. J.* 65:702–714.

Hamill, O. P., A. Marty, E. Neher, B. Sakmann, and F. J. Sigworth. 1981. Improved patch-clamp techniques for high-resolution current recording from cells and cell-free membrane patches. *Pflügers Arch.* 391:85–100.

Hodgkin, A. L., and A. F. Huxley. 1952. A quantitative description of membrane current and its application to conduction and excitation in nerve. *J. Physiol.* 117:500–544.

Kopta, C., and J. H. Steinbach. 1994. Comparison of mammalian adult and fetal nicotinic acetylcholine receptors stably expressed in fibroblasts. *J. Neurosci.* 14:3922–3933.

Lingle, C., D. Maconochie, and J. H. Steinbach. 1992. Activation of skeletal muscle nicotinic acetylcholine receptors. *J. Membr. Biol.* 126:195–217.

Maconochie, D., and J. H. Steinbach. 1992. Adult and foetal acetylcholine receptor channel opening rates. *Biophys. J.* 61:143*a*. (Abstr.)

Press, W. H., S. A. Teukolsky, W. T. Vetterling, and B. P. Flannery. 1992. Optimal (Wiener) filtering with the FFT. *In* Numerical Recipes in C. The Art of Scientific Computing. Cambridge University Press, Cambridge, U.K. 547–549.

Sigworth, F. J. 1985. Open channel noise. I. Noise in acetylcholine receptor currents suggest conformational fluctuations. *Biophys. J.* 47:709–720.

Sigworth, F. J. 1986. Open channel noise. II. A test for coupling between current fluctuations and conformational transitions in the acetylcholine receptor. *Biophys. J.* 49:1041–1046.

Sine, S. M., T. Claudio, and F. J. Sigworth. 1990. Activation of *Torpedo* acetylcholine receptors expressed in mouse fibroblasts. *J. Gen. Physiol.* 96:395–437.

Stevens, C. F. 1972. Inferences about membrane properties from electrical noise measurements. *Biophys. J.* 12:1028–1047.